Journal of Catalysis 274 (2010) 76–83

Contents lists available at ScienceDirect

Journal of Catalysis

journal homepage: www.elsevier.com/locate/jcat

Efficient and selective oxidation of benzylic alcohol by O_2 into corresponding aldehydes on a TiO_2 photocatalyst under visible light irradiation: Effect of phenyl-ring substitution on the photocatalytic activity

Shinya Higashimoto [a,*], Nobuaki Suetsugu [a], Masashi Azuma [a], Hiroyoshi Ohue [a], Yoshihisa Sakata [b]

[a] College of Engineering, Osaka Institute of Technology, 5-16-1 Omiya, Asahi-ku, Osaka 535-8585, Japan
[b] Graduate School of Science and Engineering, Yamaguchi University, 2-16-1 Tokiwadai, Ube 755-8611, Japan

ARTICLE INFO

Article history:
Received 30 April 2010
Revised 5 June 2010
Accepted 7 June 2010

Keywords:
Selective photocatalytic oxidation
Titanium dioxide
Alcohol oxidation
Benzyl alcohol
Benzaldehyde
Oxidative potential
Visible light
Electron-releasing group
Electron-withdrawing group
Resonant structure

ABSTRACT

The highly efficient and selective photocatalytic oxidation of benzyl alcohol and its derivatives substituted with $-OCH_3$, $-CH_3$, $-C(CH_3)_3$, $-Cl$, $-CF_3$ and $-NO_2$ into corresponding aldehydes has been successfully carried out on TiO_2 in the presence of O_2 under visible light irradiation. The photocatalytic activity for the formation of the aldehyde was evaluated by a pseudo-first-order reaction, and it was found that the activity is enhanced by phenyl-ring substitution with the electron-releasing groups ($-OCH_3$, $-CH_3$, $-C(CH_3)_3$) and the electron-withdrawing groups ($-Cl$, $-CF_3$ and $-NO_2$). The effects of the substituents and their orientation on the photocatalytic performance of selective oxidation reaction are discussed here. It was shown that the photocatalytic activities are influenced not only by the oxidative potentials of the reactants but also by the stability of the resonant structures of the benzylic alcohol radicals formed by oxidation with a hole, leading to further reactions to form corresponding aldehydes.

1. Introduction

The development of organic synthesis for the partial oxidation of alcohols into aldehydes or ketones has been the focus of much attention since such chemical reactions are a fundamental but significant procedure with great potential in commercial applications such as in the fragrance or pharmaceutical industries [1–3]. A number of studies have been reported on the selective catalytic oxidation of alcohol into aldehyde or ketone by O_2 using various kinds of catalysts: hydroxyapatite-supported Pd nanoclusters [4], Pd clusters embedded on mesoporous carbon [5], polymer-stabilized Au nanoclusters [6], monometallic Au [7], Au supported on CeO_2 [8] or bimetallic Au–Pd supported on TiO_2 [9], Ru supported on Al_2O_3, TiO_2 or hydroxyapatite [10–12] and carbon-supported Pt catalysts [13].

On the other hand, "green" photo-oxidation reactions have become recognized for their fundamental and applied chemical utilization of solar energy. Funyu et al. have reported the highly efficient and selective epoxidation of alkenes by photochemical oxygenation sensitized by ruthenium(II) porphyrin with water under visible light irradiation [14]. In another application, the selective photocatalytic oxidation of benzylic alcohol by O_2 into corresponding aldehydes was successfully carried out under visible light irradiation on 2,4,6-triarylpyrylium salts [15] and 9-phenyl-10-methylacridinium photocatalysts [16]. Shishido et al. have also demonstrated the photocatalytic oxidation of alcohols into corresponding aldehydes on a semiconductive Nb_2O_5 photocatalyst under solvent free conditions [17].

Meanwhile, TiO_2 photocatalysts have also been extensively utilized for such photochemical applications as H_2 production by water splitting, the degradation of volatile organic compounds (VOC), dye-sensitized solar cells, super-hydrophilic materials and organic synthesis [18–21]. Among them, the photo-oxidation of alcohol into aldehyde or ketone has been widely studied on TiO_2 [21–34]. In particular, the selective photocatalytic oxidation of benzylic alcohol by O_2 under UV-light irradiation on TiO_2 was previously reported in the gas phase [26], in acetonitrile [27,28] or in aqueous solution [29–34]. However, it is known that anatase-type TiO_2 photocatalysts have a large band-gap transition of ca. 3.2 eV, which only allows the utilization of a small percentage of the solar radiation that reaches the earth's surface. Therefore, the development of effective and highly sensitive visible light responsive TiO_2 photocatalytic systems is strongly desired. Ohno et al. have

* Corresponding author. Fax: +81 6 6957 2135.
E-mail address: higashimoto@chem.oit.ac.jp (S. Higashimoto).

0021-9517/$ - see front matter © 2010 Elsevier Inc. All rights reserved.
doi:10.1016/j.jcat.2010.06.006

reported that the photo-induced epoxidation of alkene on TiO_2 by H_2O_2 proceeds under visible light irradiation [35].

Recently, we have shown that TiO_2 exhibits efficient and selective photocatalytic oxidation of benzyl alcohol and its derivatives into corresponding aldehydes by O_2 under visible light irradiation [36,37]. These findings lead to the new development of visible light responsive photocatalystic reactions whose systems are able to utilize clean and safe solar energy. In this study, we have investigated the kinetics for the photocatalytic oxidation of benzylic alcohols substituted with $-OCH_3$, $-CH_3$, $-C(CH_3)_3$, $-Cl$, $-CF_3$ and $-NO_2$ to corresponding aldehydes by O_2 on TiO_2 under visible light irradiation. In particular, we have focused on providing an understanding of the effects of the kinds of substituents and their orientation on the efficiency of the photocatalytic oxidation reaction.

2. Experimental

2.1. Materials

All chemicals and solvents used in this study were of analytical grade and were utilized as received without further purification. Benzyl alcohol and its derivatives (*para*-benzylic alcohols substituted with –Cl and $-C(CH_3)_3$ groups and *ortho*-, *meta*- or *para*-substituted benzylic alcohols with $-OCH_3$, $-CH_3$, $-NO_2$ and $-CF_3$ groups) were obtained from Wako Pure Chemical Industries, Ltd. The photocatalyst used in this work was anatase TiO_2 (BET surface area: 320 m^2/g) obtained from Ishihara Co., Ltd. (ST-01).

2.2. Photocatalytic reactions

Photocatalytic reactions were carried out in a photoreaction cell (20 mL in volume) made of pyrex glass. The TiO_2 photocatalyst (50 mg) was suspended in acetonitrile solution (10 mL) involving the reactant (50 μmol) in the cell and the gas phase was purged by pure O_2 of 1 atmospheric pressure. The photocatalytic reaction was performed by irradiation with a blue LED lamp (OptiLED, 2.5 W, IMPACT EYE Co., Ltd.). The photo-intensity of the LED lamp was measured by an illumination meter (TMS 870, TASCO Co., Ltd.) adjusted to 1.8×10^4 lux. The energy distribution emitted from the LED lamp is shown in Fig. 1.

The quantum yield of the photocatalytic reaction was estimated under irradiation with monochromatic light of full width at half maximum (FWHM) of ca. 6.7 nm through a monochrometer (SG-100, Koken) from a 500 W Xe lamp (USHIO Co., Ltd.). The photocatalytic reaction was carried out in a photoreaction cell made of quartz with the TiO_2 photocatalyst (10 mg) suspended in acetonitrile solution (2 mL) involving benzylic alcohol (10 μmol). The photon energy was adjusted to a photon flow of 0.5–0.8 mW cm^{-2}, as measured by a power meter (ORION/PD, Ophir).

After the reaction, the catalysts were immediately separated from the solution by filtration through a 0.20-μm membrane filter (Dismic-25, Advantec). The solution was then analyzed by HPLC (Shimadzu LC10ATVP, UV–Vis detector, column: Chemcopak, mobile phase: a mixture of acetonitrile and 1.0% aqueous formic acid), and the gas phase was analyzed by GC (Model-802, Ohkura; column: porapak Q).

2.3. Characterization

Diffuse reflectance UV–Vis spectroscopic measurements were carried out using a UV–Vis spectrophotometer (UV-2200A, Shimadzu). The samples, TiO_2-adsorbed benzyl alcohol or its derivatives, were prepared in CH_3CN/0.1 M benzylic alcohol, followed by washing with acetonitrile and drying in air at room temperature.

2.4. Electrochemical measurements

Electrochemical measurements were performed with a Potentiostat/Galvanostat (HABF5001, HOKUTO DENKO). Platinum wire, saturated calomel electrodes (SCE) and a 1-mm^2 diameter glass carbon disc were used as auxiliary, reference and working electrodes, respectively. The electrolyte was bubbled vigorously by N_2 for 30 min prior to measurements. Cyclic voltammetry (CV) was measured by sweeping at 50 mV s^{-1} in CH_3CN/0.1 M $LiClO_4$/5 mM benzylic alcohol. The oxidative potentials (E_p) of the benzylic alcohols were estimated from the results of voltammogram analysis.

3. Results

3.1. Electronic properties of TiO_2-adsorbed benzylic alcohols

The UV–Vis absorption spectra were examined, and the results are shown in Fig. 2. As shown in Fig. 2a, TiO_2 by itself exhibits absorption only in the UV region, and the band-gap is estimated to be ca. 3.2 eV (ca. 380 nm) from the absorption edge of the spectrum. On the other hand, absorption in the visible region can be observed in the spectrum for the TiO_2-adsorbed benzyl alcohol, as shown in Fig. 2b, while TiO_2-adsorbed with methanol or benzene

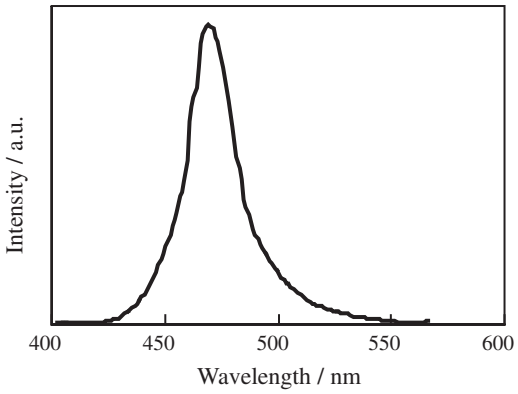

Fig. 1. Energy distribution emitted from the LED lamp (visible light) used in this experiment.

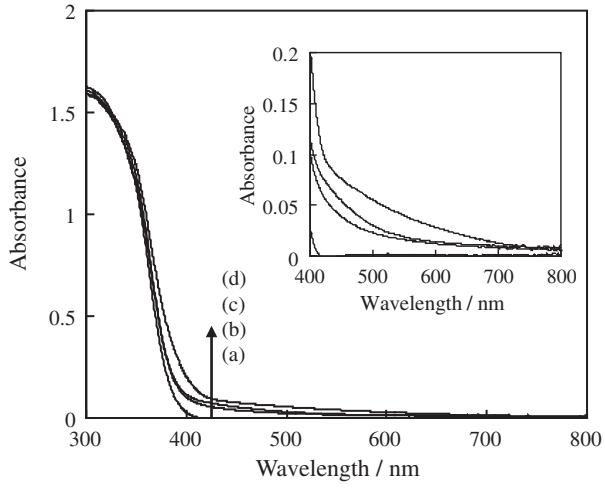

Fig. 2. UV–Vis spectra of: (a) TiO_2 by itself; and TiO_2-adsorbed (b) benzyl alcohol, (c) *p*-methoxybenzyl alcohol and (d) *p*-nitrobenzyl alcohol. Inset shows the expansion of (a)–(d).

does not exhibit absorption in the visible light region. It could, therefore, be assumed that this absorption in the visible light region was unique and was not caused by the band-gap transition from the valence band to conduction band of TiO_2. This absorption was assigned to the ligand-to-metal charge transfer (LMCT) of the surface complex formed by the interaction of benzyl alcohol with the Ti sites [38,39]. The UV–Vis spectra of the TiO_2-adsorbed benzylic alcohols were also examined. Fig. 2c and d shows the UV–Vis spectra of TiO_2-adsorbed *p*-methoxybenzyl alcohol and *p*-nitrobenzyl alcohol, respectively. Both of the spectra also show absorption in the visible light region originating with the LMCT of the surface complex. The UV–Vis spectra of the other TiO_2-adsorbed substituted benzylic alcohols used in this study were examined, and similar spectra, as shown in Fig. 2c and d, were observed. These results show that the surface complex forms by the interaction of the TiO_2 surface with the adsorbed benzylic alcohols, generating photo-absorption in the visible light region. It was observed that absorption in the visible region of the surface complex could, in fact, lead to photocatalytic reactions under visible light irradiation.

3.2. Photocatalytic oxidation of benzyl alcohol and its derivatives on TiO_2 under visible light irradiation

The oxidation of benzyl alcohol and its derivatives on a TiO_2 photocatalyst was carried out under visible light irradiation in the presence of O_2, and the results are shown in Fig. 3. It was confirmed that the oxidation reaction does not take place under visible light without a TiO_2 photocatalyst nor with a TiO_2 photocatalyst without irradiation, i.e., both TiO_2 and irradiation are required in combination for the oxidation reaction to occur. Before irradiation, a decrease in the amount of benzylic alcohol originating from its adsorption on TiO_2 was observed. After confirming the equilibrium adsorption of benzylic alcohol on TiO_2, the light was turned on. As shown in Fig. 3a, the amount of benzyl alcohol decreased with an increase in irradiation time while that of benzaldehyde increased with the formation of only negligible amounts of benzoic acid or CO_2. It should be noted that these reactions immediately ceased when the light was turned off. When the light was then turned back on, the reactions immediately proceeded again. These results indicate that they are not an auto-oxidative chain reaction, but a photo-responsive reaction system. After irradiation for 240 min, the benzyl alcohol was completely converted into benzaldehyde with high selectivity (>99%) without further oxidation into benzoic acid or CO_2.

The photocatalytic oxidation of various kinds of benzylic alcohol substituted with $-OCH_3$, $-CH_3$, $-C(CH_3)_3$, $-Cl$, $-CF_3$ and $-NO_2$ was also investigated, and the results are shown in Fig. 3b–o. Here, the reactants, as shown above, were classified into two categories: category A includes benzylic alcohols substituted with such electron-releasing groups as $-OCH_3$, $-CH_3$, $-C(CH_3)_3$, as shown in Fig. 3b–h; while category B includes benzylic alcohols substituted with such electron-withdrawing groups as $-Cl$, $-CF_3$ and $-NO_2$, as shown in Fig. 3i–o. For all of the photocatalytic reaction systems, as shown in Fig. 3, it was found that the selective photocatalytic oxidation of benzylic alcohols by O_2 into corresponding aldehydes was successfully carried out on TiO_2 under visible light irradiation, while an induction period was appeared with its time dependence on the kind of substituent. It was, thus, confirmed that benzylic alcohols in both categories A and B are converted into corresponding aldehydes with high conversion (>99%) and with high selectivity (>99%). However, the total mass balance was less than 100% in the photocatalytic oxidation of benzylic alcohols belonging to categories A and B after the reactions were completed, as shown in Fig. 3. Here, the uptakes of various kinds of aldehydes on TiO_2 were characterized after equilibrium adsorption in the dark. Consequently, it was confirmed that the total mass balance after the reactions could be explained by the equilibrium adsorption of the aldehydes on the TiO_2 surface (Table S1, Supplementary material).

3.3. Quantum yields of the photocatalytic selective oxidation of benzyl alcohol and its derivatives on TiO_2

Fig. 4 shows the quantum yields (Φ) for the photocatalytic oxidation of (a) benzyl alcohol, (b) *p*-methoxybenzyl alcohol and (c) *p*-nitrobenzyl alcohol into corresponding aldehydes on TiO_2 as a function of the photo-irradiation wavelength. The quantum yield (Φ) is defined in the following Eq. (1):

$$\Phi = \frac{\text{amount of product formed}}{\text{amount of photons absorbed}} \times 100 \quad (1)$$

The photo-response for the oxidation of benzyl alcohol into benzaldehyde was confirmed up to ca. 700 nm, and the quantum yields were estimated to be ca. 4.3% under photo-irradiation at 500 nm, ca. 5.5% at 460 nm and ca. 13.8% at 440 nm, as shown in Fig. 4a. These results clearly indicate that visible light absorption plays a significant role in the photocatalytic selective oxidation of benzyl alcohol into benzaldehyde. The quantum yields for the oxidation of *p*-methoxybenzyl alcohol into aldehyde are estimated to be ca. 6.8% under photo-irradiation at 500 nm, ca. 17% at 460 nm and ca. 29.1% at 440 nm, as shown in Fig. 4b, while those of *p*-nitrobenzyl alcohol into aldehyde are estimated to be ca. 13.4% under photo-irradiation at 500 nm, ca. 39.2% at 460 nm and ca. 67.4% at 440 nm, as shown in Fig. 4c. Thus, it was noted that the quantum yields for the photocatalytic oxidation of benzylic alcohols substituted with $-OCH_3$ and $-NO_2$ are significantly higher than those of benzyl alcohol.

3.4. Kinetics of the photocatalytic oxidation of benzyl alcohol and its derivatives

Characterization studies of the photocatalytic activity for the oxidation of benzylic alcohol into corresponding aldehydes were carried out by examining the reaction rate constants. If the photo-formed aldehyde increases without the induction period, the photocatalytic activity can be simply evaluated by the first-order kinetics. Here, it is considered that the induction period (0–2000 s) as shown in Fig. 3 may be attributed to a surface reconstruction between benzylic alcohol and TiO_2 during photo-irradiation, leading to the formation of the more active surface structure than the initial state. Therefore, the apparent reaction rate constant (k) was confirmed to simulate the part of an increment except for the induction period by the first-order kinetic analysis.

Under conditions of sufficient O_2 concentration during the photocatalytic reactions, the reaction kinetics were ruled by the following pseudo-first-order Eq. (2) or (3).

$$k(t_0 - t) = \ln\{a_0/(a_0 - x)\} \quad (2)$$

$$x = a_0\{1 - \exp k(t_0 - t)\} \quad (3)$$

Here, a_0, x, k, t and t_0 represent the amounts of added reactant molecules (50 μmol), photo-formed corresponding aldehyde, the apparent reaction rate constant, reaction time, and induction period, respectively. For example, except for the induction period, $\ln\{a_0/(a_0 - x)\}$ against t for the oxidation of benzyl alcohol exhibits a linear relationship, as shown in Fig. 5I. The k and t_0 values are obtained from the slope and interpolated value at the x-axis of the linear line. Using set k and t_0 values, the amount of photo-formed

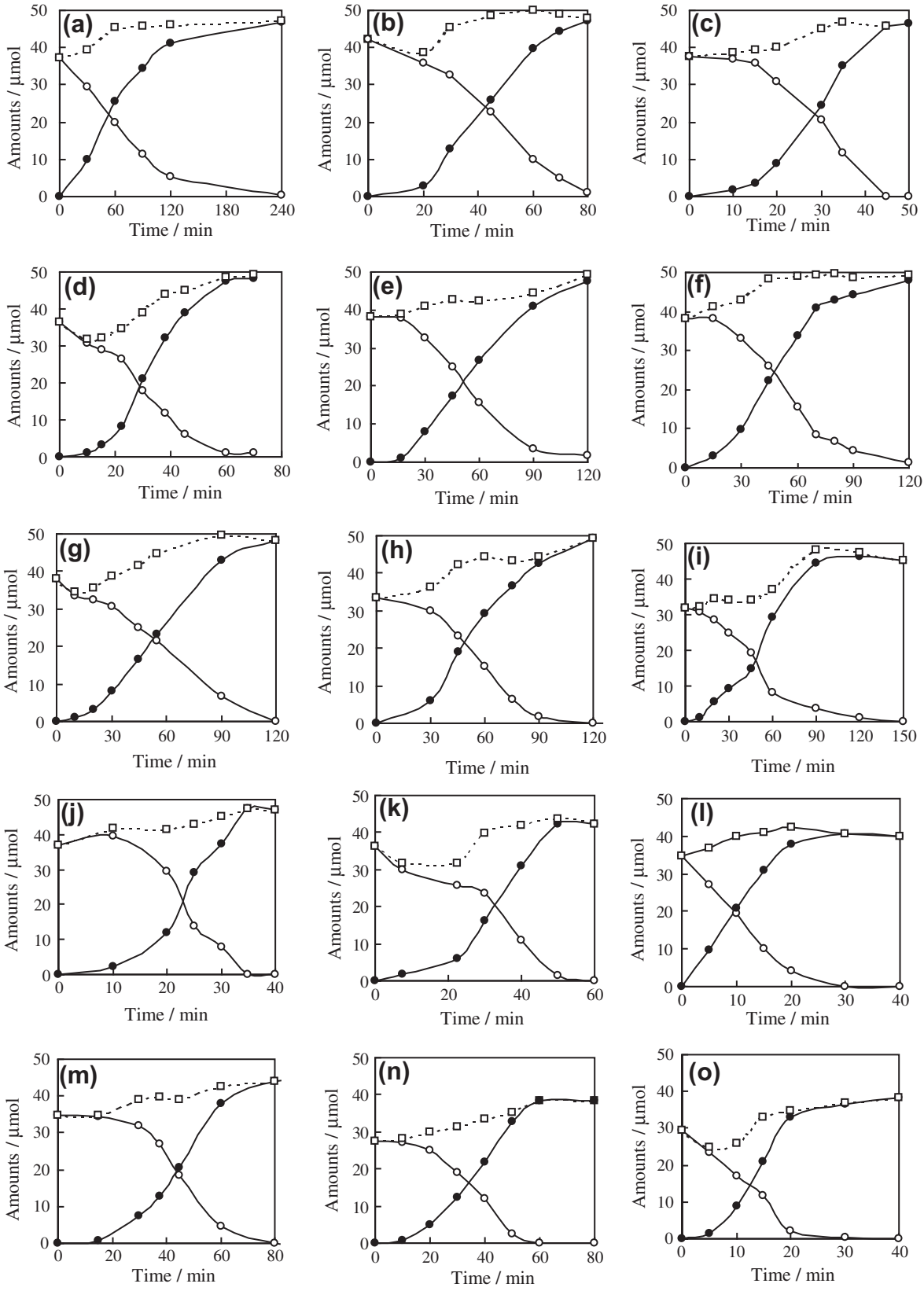

Fig. 3. Photocatalytic oxidation of various kinds of benzylic alcohols on TiO_2 (50 mg) under visible light irradiation. The initial amount of alcohol added to the reaction cell was 50 μmol. Amounts of (○) alcohol; (●) aldehyde; and (□) total alcohol and aldehyde. Reactants: benzylic alcohols substituted with the following groups: (a) -H, (b) *o*-OCH_3, (c) *m*-OCH_3, (d) *p*-OCH_3, (e) *o*-CH_3, (f) *m*-CH_3, (g) *p*-CH_3, (h) *p*-$(CH_3)_3$, (i) *p*-Cl, (j) *o*-CF_3, (k) *m*-CF_3, (l) *p*-CF_3, (m) *o*-NO_2, (n) *m*-NO_2 and (o) *p*-NO_2.

benzaldehyde (x) was simulated, as shown in Fig. 5II. The induction period (t_0) and the apparent reaction rate constants (k) for the oxidation of different kinds of benzylic alcohols were thus estimated, as shown in Fig. S1. The relationship between the photocatalytic activities and the oxidative potentials of benzylic alcohols will be discussed in the following section.

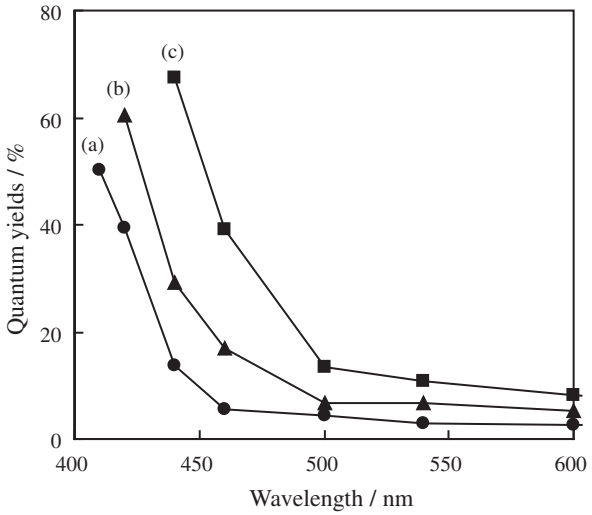

Fig. 4. Quantum yields for the photocatalytic oxidation of (a) benzyl alcohol, (b) *p*-methoxybenzyl alcohol and (c) *p*-nitrobenzyl alcohol into corresponding aldehydes on TiO_2 under light irradiation of various wavelengths.

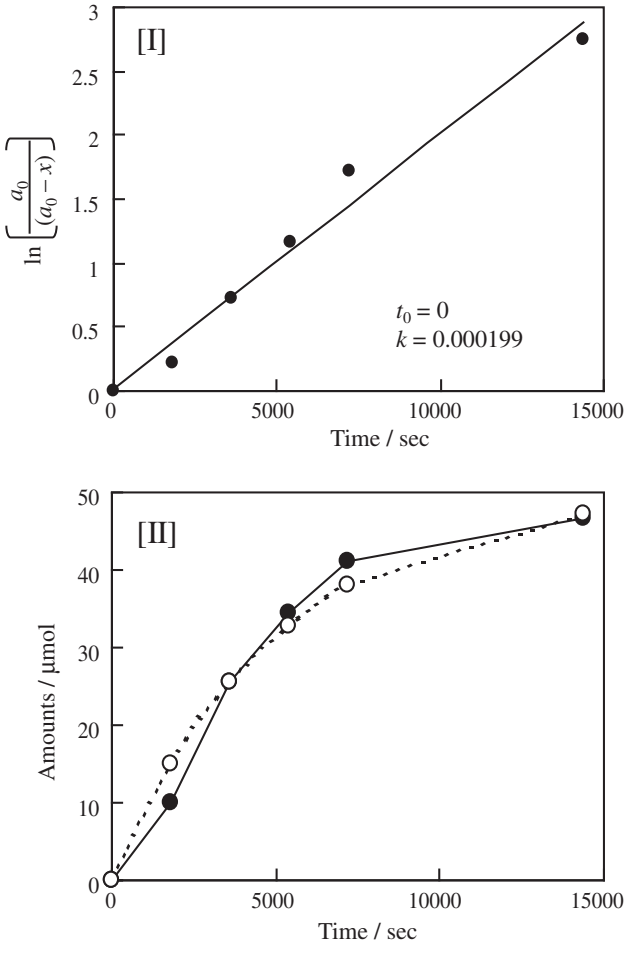

Fig. 5. Plots [I] for $\ln\{a_0/(a_0 - x)\}$ against the time for the formation of benzaldehyde. Plots [II] for the amount of photo-formed benzaldehyde with experiment (●) and its simulation (○).

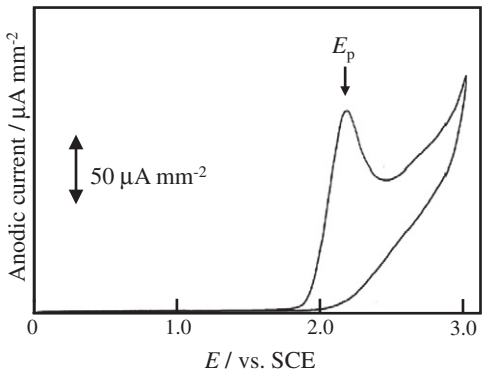

Fig. 6. Cyclic voltammogram of benzyl alcohol. The first oxidative potential (E_p) of the benzyl alcohol is shown by an arrow.

3.5. Relationship between the photocatalytic activities and the oxidative potentials of benzylic alcohols on TiO_2 under visible light irradiation

The cyclic voltammogram of benzyl alcohol was recorded in the range of 0–3.0 V vs. SCE in the dark, and the results are shown in Fig. 6. This voltammogram exhibits an irreversible curve and first oxidative potential (E_p) of the benzyl alcohol at ca. +2.16 V vs. SCE, as shown in Fig. 6. It is known that the E_p of benzyl alcohol is attributable to the one-electron oxidation from the phenyl-ring [40]. Similarly, the cyclic voltammogram of various kinds of benzylic alcohols have been recorded (Fig. S2, Supplementary material) and the E_p for these are listed in Table 1. It was observed that the E_p is strongly influenced by phenyl-ring substitution: the reactant molecules in category A exhibit lower E_p in the range of 1.66–2.08 V, while those in category B have higher E_p in the range of 2.17–2.80 V than benzyl alcohol (+2.16 V), as shown in Table 1. Moreover, it can be seen that the *ortho*-, *meta*- and *para*-oriented methoxybenzyl alcohol and nitrobenzyl alcohol showed E_p at 1.76, 1.80 and 1.66 V for methoxybenzyl alcohol, and 2.80, 2.80 and 2.80 V vs. SCE for nitrobenzyl alcohol, respectively. Thus, it was confirmed that the E_p of benzylic alcohols are significantly influenced by different kinds of substituents, not so by their orientation. Fig. 7 shows the apparent reaction rate constant (k) as a function of the E_p. It was observed that the photocatalytic activity was not governed by the Hammett rule, i.e., substitution with the electron-releasing groups $-OCH_3$, $-CH_3$, $-C(CH_3)_3$ in category A as well as with the electron-withdrawing groups –Cl, $-CF_3$ and $-NO_2$ in category B increased the photocatalytic activity of benzyl alcohol, as shown in Fig. 7.

Table 1
Oxidative potentials (E_p) of benzyl alcohol and its derivatives.

X	V (vs. SCE) 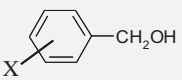		
H	2.16		
	(*ortho*-	*meta*-	*para*-)
Category A			
OCH_3	1.76	1.80	1.66
CH_3	2.08	2.08	1.95
$C(CH_3)_3$	–	–	2.06
Category B			
Cl	–	–	2.17
CF_3	2.70	2.65	2.75
NO_2	2.80	2.80	2.80

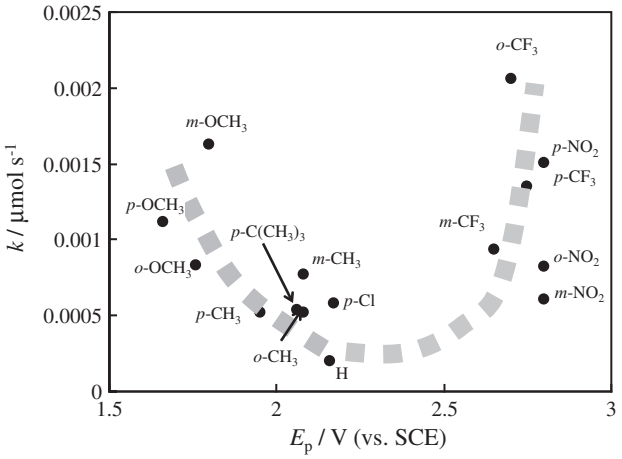

Fig. 7. Relationship between the apparent reaction rate constants (k) for the photocatalytic oxidation of benzylic alcohols and their oxidative potentials (E_p). The substituents of the benzylic alcohols are shown in this figure.

4. Discussion

The photocatalytic oxidation of benzylic alcohols into corresponding aldehydes was observed to proceed on TiO_2 with high efficiency and selectivity without further oxidation into benzoic acid or CO_2 under visible light irradiation. Scheme 1 shows the reaction mechanism for the photocatalytic oxidation of benzylic alcohol by O_2 on TiO_2 under visible light irradiation. This scheme is derived from a well-known mechanism for the electrochemical oxidation of benzyl alcohols into aldehydes [41].

In this photocatalytic system, the surface complexes, which are formed by the interaction of the $-CH_2OH$ group of molecular benzyl alcohol with the TiO_2 surface, induce absorption in the visible light region [36,37]. Therefore, upon visible light irradiation, the surface complex is photo-excited to form electrons (e^-) and holes (h^+). It should be noted that they were not photo-induced by direct excitation of the TiO_2 band-gap.

On the other hand, the photocatalytic oxidation of benzyl alcohol under pure O_2 (1 atm), air and N_2 were examined. It was found that the efficiency for the photocatalytic oxidation of benzyl alcohol depends on the concentration of O_2: the photocatalytic activity was higher in the presence of pure O_2 than in air, and almost no activity was observed under N_2. Furthermore, the first-order isotope effect shows that the C–D bond of α, α-d2 benzyl alcohol is cleaved more slowly than the C–H bond of normal benzyl alcohol

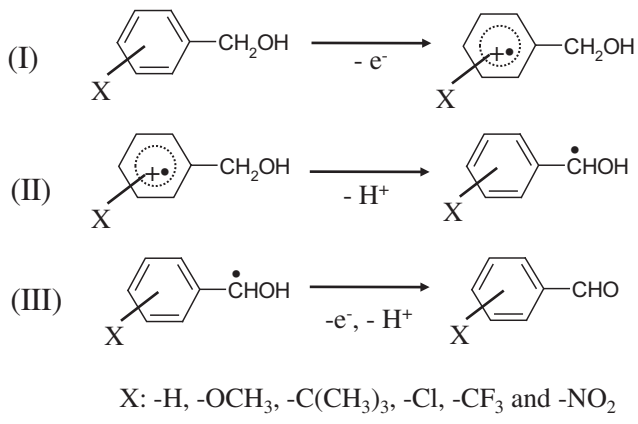

Scheme 1. Reaction mechanism for the photocatalytic oxidation of benzylic alcohol by O_2 on TiO_2 under visible light irradiation.

with a ratio of k_{C-H}/k_{C-D} at ≈3.9 [36]. This result suggests that the photo-excitation of the surface complex plays an important role in the abstraction of the α-hydrogen atom from the $-CH_2OH$ group as a rate-determining step. It can be, therefore, assumed that the abstraction of H atom, as shown in Schemes 1I and II, is one of the important steps, while the presence of O_2 as an electron acceptor seems to assist de-protonation and elimination of the electron from benzyl alcoholic radical cation as shown in Scheme 1II and III.

As shown in Fig. 7, the effect of the substituent on the photocatalytic activity as a function of the E_p of benzylic alcohols shows the U-shaped curve, which is not governed by the Hammett rule. It is known that the Hammett rule is often applied to the ionic reaction, not to the photo-induced radical reaction. How can the relationship between the photocatalytic activity and the E_p in Fig. 7 be explained? It was first confirmed that the photocatalytic activity does not directly depend on the amount of adsorbed benzylic alcohol or visible light absorbance of the TiO_2-adsorbed benzylic alcohol (Figs. S3 and S4, Supplementary material).

In order to understand the contribution of the photo-generated hole, Ag^+ was applied as an electron scavenger. Fig. 8 shows the UV–Vis spectra of TiO_2 after visible light irradiation for 60 s in the presence of the reactants: (a) *p*-nitrobenzyl alcohol, (b) *p*-(trifluoromethyl)benzyl alcohol, (c) benzyl alcohol, (d) *p*-methylben-

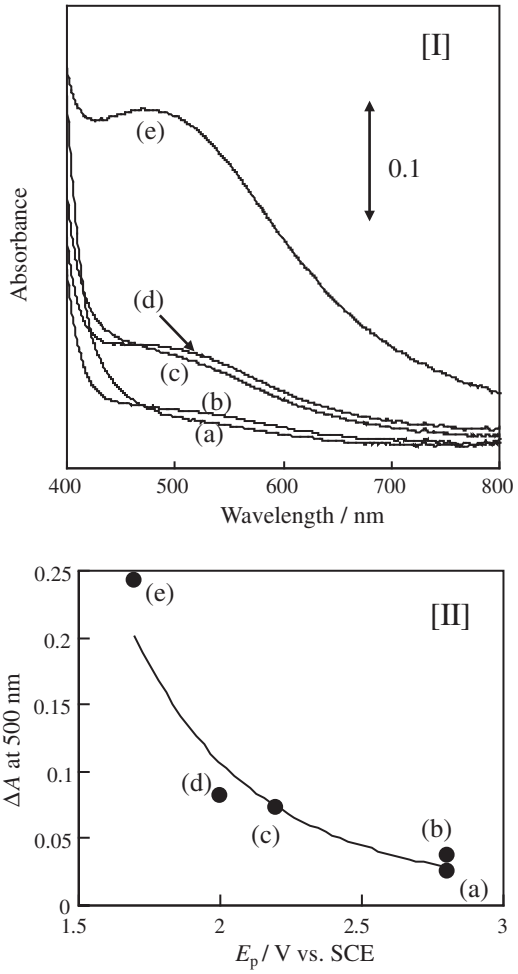

Fig. 8. UV–Vis spectra [I] of TiO_2 after 60 s visible light irradiation in the presence of Ag^+ ions (50 μmol) with the benzylic alcohols (50 μmol), and the absorbance, ΔA [II] as a function of E_p of benzylic alcohol. The benzylic alcohols used in this experiment are (a) *p*-nitrobenzyl alcohol, (b) *p*-(trifluoromethyl)benzyl alcohol, (c) benzyl alcohol, (d) *p*-methylbenzyl alcohol and (e) *p*-methoxybenzyl alcohol. The ΔA was estimated by subtracting the un-irradiated spectrum from the photo-irradiated one.

zyl alcohol and (e) *p*-methoxybenzyl alcohol, with Ag^+ ions instead of O_2. As shown in Fig. 8I-c, when visible light irradiation of TiO_2 was carried out in the presence of benzyl alcohol and Ag^+ ions under N_2 atmosphere, a broad absorption at ca. 400–800 nm could be observed. This absorption at ca. 400–800 nm is attributed to the Ag particles [42]. It should be noted that the Ag^+ ions by itself could not be directly reduced by the reactant molecules but through the TiO_2 surface, suggesting that the electron transfer takes place by way of the TiO_2 surface to the electron scavenger such as O_2. It was also shown that the band intensity attributed to Ag depends on the kinds of adsorbed benzylic alcohols, and their band intensities were observed in the following order: *p*-methoxybenzyl alcohol ≫ *p*-methylbenzyl alcohol > benzyl alcohol > *p*-(trifluoromethyl)benzyl alcohol > p-nitrobenzyl alcohol after irradiation. Fig. 8II shows the relationship between the absorbance (ΔA) at 500 nm, as shown in Fig. 8I, and the E_p of the reactants. From Fig. 8II, it was observed that the ΔA decreases with an increase in the value of E_p of the reactant molecules. This indicates that the lower the E_p value of the reactants interacting with TiO_2, the higher the reducibility of the Ag^+ ions. In other words, one-electron oxidation from benzylic alcohol with low E_p takes place more efficiently by a photo-induced hole. However, the relationship between the photocatalytic activity and E_P for the benzylic alcohols belonging to both categories A and B, as shown in Fig. 7, has yet to be fully understood by the one-electron oxidizability of benzylic alcohols.

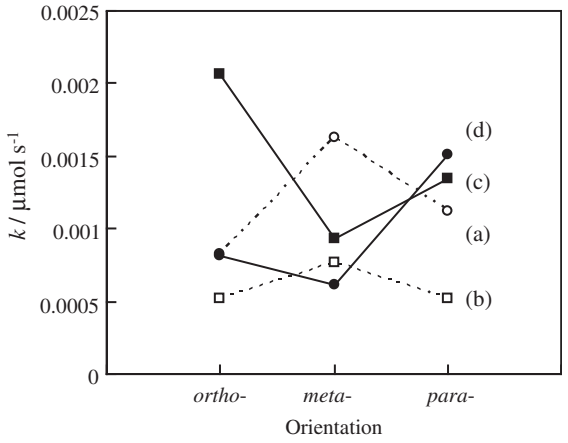

Fig. 9. Apparent reaction rate constants (k) for the photocatalytic oxidation of benzylic alcohols substituted with *ortho*-, *meta*- and *para*-oriented (a) $-OCH_3$, (b) $-CH_3$, (c) $-CF_3$ and (d) $-NO_2$ into corresponding aldehydes.

According to a previous report [43], it is known that the rate constant for α-C–H de-protonation from benzyl alcohol (and more generally alkylaromatic) radical cations decrease by increasing the stability of the radical cation. As shown in Scheme 1II, de-protonation from the radical cations is influenced by the substituents. In particular, the radical cations de-stabilized by such electron-withdrawing groups as $-CF_3$ and $-NO_2$ may favorably promote de-protonation, followed by de-protonation and elimination of an electron from the benzylic alcohol radical, as shown in Scheme 1III.

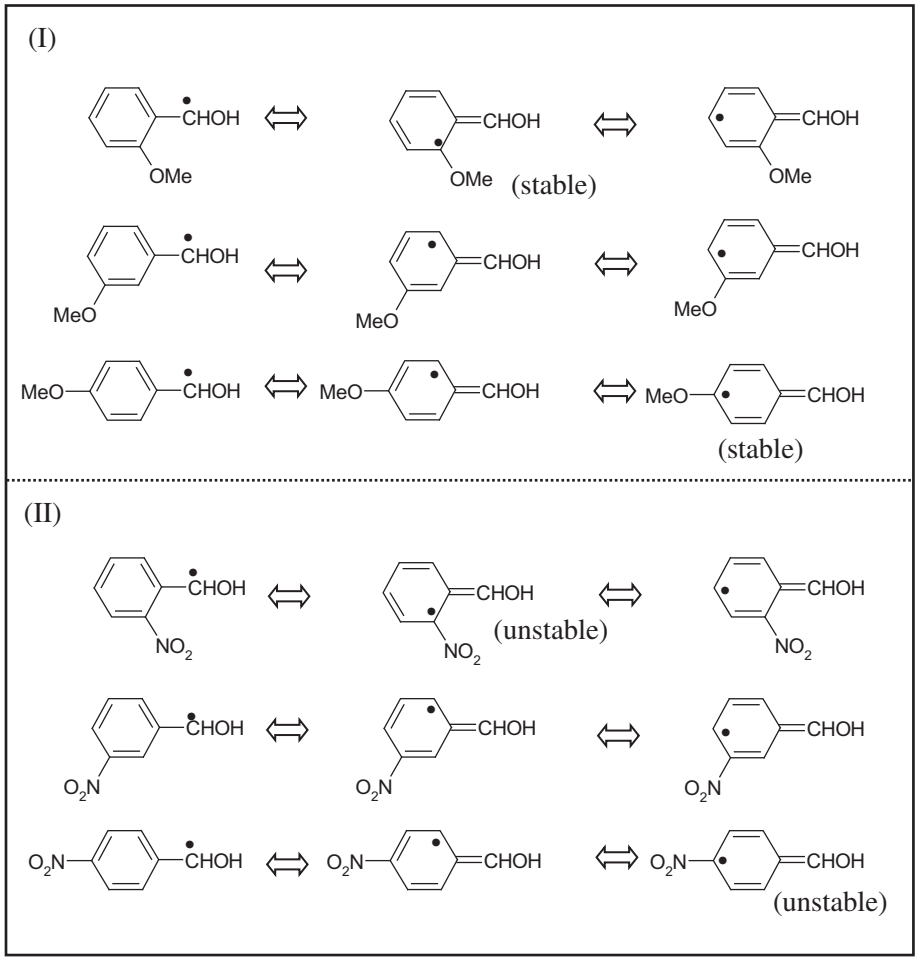

Scheme 2. Resonant structures of benzylic alcohol radicals belonging to I and II.

Fig. 9 shows the effect of the electronic properties by the *ortho*-, *meta*- and *para*-orientation on the photocatalytic activity for the oxidation of benzylic alcohols substituted with (a) $-OCH_3$, (b) $-CH_3$, (c) $-CF_3$ and (d) $-NO_2$ into corresponding aldehyde. It was observed that methoxybenzaldehyde and methylbenzaldehyde in *meta*-orientation are photo-formed more efficiently than in *ortho*- and *para*-orientation, while nitrobenzaldehyde and (trifluoromethyl)-benzaldehyde in *ortho*- and *para*-orientation are formed more efficiently than in *meta*-orientation.

Here, Scheme 2I and II proposes the resonant structures of the methoxybenzyl alcohol radicals and nitrobenzyl alcohol radicals as representative of categories A and B, respectively. The resonant structures of the methoxybenzyl alcohol radicals were found to be more stabilized in *ortho*- and *para*-orientation than in *meta*-orientation, as shown in Scheme 2I. Assuming that the un-stabilized resonant structures of the methoxybenzyl alcohol radicals efficiently promote further reactions, the methoxybenzaldehyde in *meta*-orientation is more efficiently formed than in *ortho*- and *para*-orientation. On the other hand, the resonant structures of the nitrobenzyl alcohol radicals were found to be more de-stabilized in *ortho*- and *para*-orientation than in *meta*-orientation, as shown in Scheme 2II. Therefore, the nitrobenzaldehyde in *ortho*- and *para*-orientation is more efficiently formed than in *meta*-orientation. The effect of the orientation on the photocatalytic activity could, thus, be clearly explained by the stability of the resonant structures of the benzylic alcohol radicals, i.e., the resonant structures of the radicals in *meta*-orientation for category A and in *ortho*- and *para*-orientation for category B enhance destabilization, leading to further reactions to form corresponding aldehydes.

5. Conclusions

The photocatalytic oxidation of benzyl alcohol and its derivatives on TiO_2 in the presence of O_2 were investigated under visible light irradiation. It was found that the selective photocatalytic oxidation of benzylic alcohols into corresponding aldehydes proceeded with high conversion of >99% and high selectivity of >99%. These visible light–induced reactions were attributed to the oxidation of the surface complex formed by the interaction of benzylic alcohol with TiO_2.

The photocatalytic activity of the benzylic alcohols was enhanced by phenyl-ring substitution with the electron-releasing groups ($-OCH_3$, $-CH_3$, $-C(CH_3)_3$) as well as the electron-withdrawing groups ($-Cl$, $-CF_3$ and $-NO_2$). These phenomena could be explained by a combination of the oxidizability with the phenyl-ring of benzylic alcohol to form the benzylic alcohol radical cation and the efficiency for α-C–H de-protonation from the radical cation. It was also shown that the orientation of the phenyl-ring substituents influences the photocatalytic activity, i.e., the more de-stabilized the resonant structures of the benzyl alcoholic radicals in *meta*-orientation of category A and in *ortho*- and *para*-orientation of category B, the more efficient the conversion into corresponding aldehydes. To the best of our knowledge, this is the first report characterizing the effect of the substituents for the photocatalytic oxidation of benzylic alcohol into corresponding aldehydes under visible light irradiation. The results of this work are useful in the utilization of clean and safe solar energy while practical studies for photocatalytic organic synthesis are presently underway.

Appendix A. Supplementary data

Supplementary data associated with this article can be found, in the online version, at doi:10.1016/j.jcat.2010.06.006.

References

[1] G.J. Brink, I.W.C.E. Arends, R.A. Sheldon, Science 287 (2000) 1636.
[2] T. Mallat, A. Baiker, Chem. Rev. 104 (2004) 3037.
[3] M. Nechab, C. Einhorn, J. Einhorn, Chem. Commun. (2004) 1500.
[4] K. Mori, T. Hara, T. Mizugaki, K. Ebitani, K. Kaneda, J. Am. Chem. Soc. 126 (2004) 10657.
[5] A.H. Lu, W.C. Li, Z. Hou, F. Schueth, Chem. Commun. 10 (2007) 1038.
[6] H. Tsunoyama, H. Sakurai, N. Negishi, T. Tsukuda, J. Am. Chem. Soc. 127 (2005) 9374.
[7] M. Turner, V.B. Golovko, O.P.H. Vaughan, P. Abdulkin, A. Berenguer-Murcia, M.S. Tikhov, B.F.G. Johnson, R.M.G. Lambert, Nature 454 (2008) 981.
[8] A. Abad, C. Almela, A. Corma, H. Garcia, Chem. Commun. (2006) 3178.
[9] D.I. Enache, J.K. Edwards, P. Landon, B. Solsona-Espriu, A.F. Carley, A.A. Herzing, M. Watanabe, C.J. Kiely, D.W. Knight, G.J. Hutchings, Science 311 (2006) 362.
[10] K. Yamaguchi, N. Mizuno, Angew. Chem. Int. Ed. 41 (2002) 4538.
[11] K. Yamaguchi, J.W. Kim, J. He, N. Mizuno, J. Catal. 268 (2009) 343.
[12] K. Yamaguchi, K. Mori, T. Mizugaki, K. Ebitani, K. Kaneda, J. Am. Chem. Soc. 122 (2000) 7144.
[13] Y.H. Ng, S. Ikeda, T. Harada, Y. Morita, M. Matsumura, Chem. Commun. (2008) 3181.
[14] S. Funyu, T. Isobe, S. Takagi, D.A. Tryk, H. Inoue, J. Am. Chem. Soc. 125 (2003) 5734.
[15] A. Tashiro, A. Mitsuishi, R. Irie, T. Katsuki, Syn. Lett. 12 (2003) 1868.
[16] K. Ohkubo, K. Suga, S. Fukuzumi, Chem. Commun. 19 (2006) 2018.
[17] T. Shishido, T. Miyatake, K. Teramura, Y. Hitomi, H. Yamashita, T. Tanaka, J. Phys. Chem. C 113 (2009) 18713.
[18] M. Kitano, K. Iyatani, K. Tsujimaru, M. Matsuoka, M. Takeuchi, M. Ueshima, J.M. Thomas, M. Anpo, Top. Catal. 49 (2008) 24.
[19] M. Grätzel, J. Photochem. Photobiol. C: Photochem. Rev. 4 (2003) 145.
[20] A. Fujishima, T.N. Rao, D.A. Tryk, J. Photochem. Photobiol. C: Photochem. Rev. 1 (2000) 1.
[21] M.A. Fox, M.T. Dulay, Chem. Rev. 93 (1993) 341.
[22] J.D.F. Ollis, W.H. Rulkens, H. Bruning, Water Res. 33 (1998) 669.
[23] D.S. Muggli, J.T. Mccue, J.L. Falconer, J. Catal. 173 (1998) 470.
[24] J.L. Falconer, K.A. Magrini-Bair, J. Catal. 179 (1998) 171.
[25] F.H. Hussein, G. Pattenden, R. Rudham, J.J. Russell, Tetrahedron Lett. 25 (1984) 3363.
[26] U.R. Pillai, E. Sahle-Demessie, J. Catal. 211 (2002) 434.
[27] O.S. Mohamed, A.E.M. Gaber, A.A. Abdel-Wahab, J. Photochem. Photobiol. A 148 (2002) 205.
[28] S. Farhadi, M. Afshari, M. Maleki, Z. Badazadeh, Tetrahedron Lett. 46 (2005) 8483.
[29] S. Yurdakal, G. Palmisano, V. Loddo, V. Augugliaro, L. Palmisano, J. Am. Chem. Soc. 130 (2008) 1568.
[30] V. Augugliaro, T. Caronna, V. Loddo, G. Marci, G. Palmisano, L. Palmisano, S. Yurdakal, Chem. A. Eur. J. 14 (2008) 4640.
[31] G. Palmisano, S. Yurdakal, V. Augugliaro, V. Loddo, L. Palmisano, Adv. Synth. Catal. 349 (2007) 964.
[32] G. Palmisano, M. Addamo, V. Augugliaro, T. Caronna, E. Garcia-Lopez, V. Loddo, L. Palmisano, Chem. Commun. (2006) 1012.
[33] M. Addamo, V. Augugliaro, M. Bellardita, A. Di Paola, V. Loddo, G. Palmisano, L. Palmisano, S. Yurdakal, Catal. Lett. 126 (2008) 58.
[34] S. Yurdakal, G. Palmisano, V. Loddo, O. Alagoez, V. Augugliaro, L. Palmisano, Green Chem. 11 (2009) 510.
[35] T. Ohno, Y. Masaki, S. Hirayama, M. Matsumura, J. Catal. 204 (2001) 163.
[36] S. Higashimoto, N. Kitao, N. Yoshida, T. Sakura, M. Azuma, H. Ohue, Y. Sakata, J. Catal. 266 (2009) 279.
[37] S. Higashimoto, K. Okada, T. Morisugi, A. Nakagawa, M. Azuma, H. Ohue, T.H. Kim, M. Matsuoka, M. Anpo, Top. Catal. 53 (2010) 578.
[38] Y. Wang, K. Hang, N.A. Anderson, T. Lian, J. Phys. Chem. B 107 (2003) 9434.
[39] T. Tachikawa, S. Tojo, M. Fujitsuka, T. Majima, Langmuir 20 (2004) 2753.
[40] D.T. Sawyer, A. Sobkowiak, J.L. Roberts (Eds.), Electrochemistry for Chemists, John Wiley & Sons, Inc., New York, 1996, p. 369 (translated in Japanese).
[41] H. Lund, O. Hammerich (Eds.), Organic Electrochemistry, Marcel Dekker, New York, 2001, p. 611.
[42] T. Hirakawa, P.V. Kamat, Langmuir 20 (2004) 5645.
[43] B. Branchi, M. Bietti, G. Ercolani, M.A. Izquierdo, M.A. Miranda, L. Stella, J. Org. Chem. 69 (2004) 8874.